Research Report

Vibration-reducing Motor Control for Hybrid Vehicles

Yoshiaki Ito, Shuji Tomura, Kazunari Moriya

ハイブリッド自動車の制振制御

伊藤嘉昭，戸村修二，守屋一成

Abstract

This paper describes a motor control method that is designed to reduce vibration in hybrid vehicles (HV).

Vibration that can degrade ride comfort occurs in the following situations.

1) At engine start/stop

In an HV, engine start/stop occurs frequently in the interests of reducing fuel consumption and emissions. This vibration occurs independently of the driver's actions.

2) During rapid acceleration/deceleration

The vibration increases considerably because the electric motor torque can be increased/decreased more rapidly than that of the internal combustion engine.

To address these problems, we have designed two types of controllers. The first controller addresses the problem of engine torque ripple that is caused by the compression reaction force and the pumping pressure in the cylinders. The second controller has been designed to suppress torsional vibration in the drivetrain, which is caused by traction torque ripples or rapid increases/decreases in the traction torque.

Both controllers are realized in software. Practical experiments have shown that the proposed motor controllers reduce vibration and improve ride comfort.

Keywords Hybrid vehicle, Motor, Engine, Control, Vibration, Ride comfort

要　旨

本研究は，ハイブリッド自動車 (HV) で発生する車両振動の低減を目的に開発したモータ制御手法に関するものである。

ここでは，以下の2状況で発生する車両振動について考える。

1) エンジン始動／停止時

燃費やエミッションの向上のため，HVでは頻繁に繰り返される。ドライバの操作とは無関係に発生する振動であるため，違和感を生じる。

2) 高トルク応答のモータで急加減速する時

これらの振動は，エンジントルクの脈動や駆動トルクの急速な変化によって発生する。

そこで，エンジントルクの脈動を駆動系に伝達させないモータ制御手法と，駆動系のねじれ振動を低減するモータ制御手法とを開発した。開発した制御手法は既存のセンサだけを利用しており，ソフトウェアを変更するだけで実現可能な手法である。

実車試験の結果，上記の状況で発生する車両振動をモータ制御によって低減できることを確認した。不快な振動が低減されるため，乗り心地も良くなることを確認した。

キーワード　ハイブリッド自動車，モータ，エンジン，制御，振動，乗り心地

1. Introduction

The internal combustion engine (ICE) of a hybrid vehicle (HV) is started and stopped frequently in order to improve fuel consumption and reduce emissions. Unfortunately, the vibration associated with this starting/stopping degrades the ride comfort. A characteristic of this vibration is that it is not related to the driver's actions. An HV can adjust the traction torque of its electric motor more quickly than is possible in conventional ICE vehicles. As a result, an excellent torque response is also one of the features of an HV. This rapid torque change causes vibration, however, which also leads to a poorer ride comfort.

To date, several methods of reducing these types of vibration have been investigated.[1-7] The goal of this study was to develop a motor control method that would reduce the vibration that occurs in the above situations and therefore improve the ride comfort.

2. Powertrain of an HV

Figure 1 shows the construction of an HV powertrain.[8] The HV has a gasoline engine, a motor and a generator. The engine is connected to the planetary carrier of the planetary gear set via a flywheel and a damper, while the generator and the motor are connected to the sun gear and the ring gear. The traction torque, which is the sum of the engine torque τ_e and motor torque τ_M, is transmitted from the ring gear to the drive shaft via a reduction gear and differential gear.

A characteristic of this construction, from the viewpoint of vibration, is that there are no separation devices like a clutch, such that the engine and motor are always connected to the driving wheels. So, the traction torque generated by the engine and the motor is always transmitted to the driving wheels.

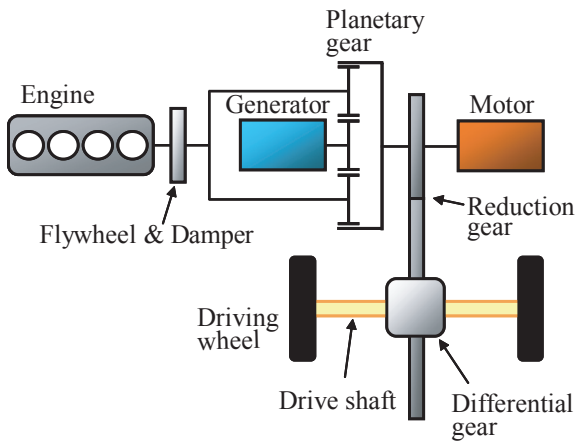

Fig. 1 HV powertrain.

3. Vibration arising in the HV Powertrain

Vibration that is characteristic of an HV occurs when the engine starts/stops and upon rapid acceleration/deceleration. In this chapter, the cause and effect of the vibration are described using engine start as an example.

The generator acts as a starter to start the engine. The ignition is activated once the engine reaches the prescribed speed. **Figure 2** shows the floor acceleration, which indicates the vibration, generator torque, and engine speed.

The vibration at engine start can be divided into two modes.[1] Before the ignition is activated, the compression reaction force and pumping pressure in the cylinders cause vibration. Once the ignition is

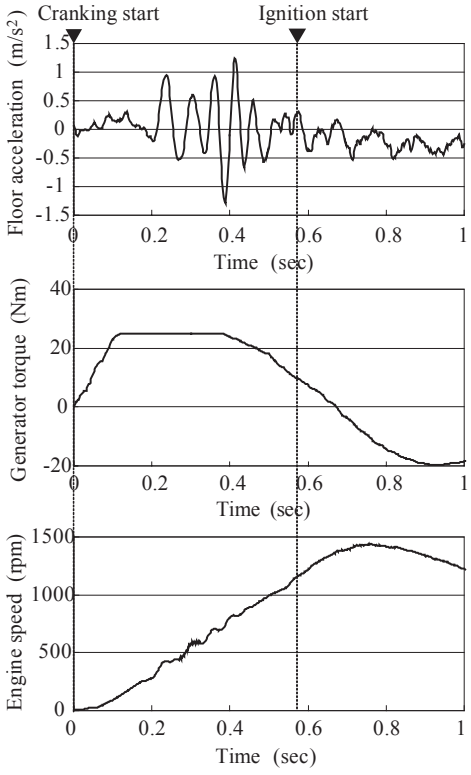

Fig. 2 Response at engine start.

activated, vibration occurs as a result of the rapid engine torque increment caused by the combustion.

At engine stop and upon rapid acceleration/deceleration, vibration occurs for similar reasons.

4. Vibration-reducting control

This chapter describes the design of a motor control method that reduces vibration in the powertrain. This vibration-reducting control method consists of two controllers. The first aims to control the engine torque ripple that is caused by the compression reaction force and the pumping pressure in the cylinders. The second aims to control torsional vibration in the drivetrain that is caused by traction torque ripple or a rapid increase/decrease in the traction torque.

4. 1 Engine torque ripple control

4. 1. 1 Design concept

The design objective of the first controller was to prevent engine torque ripple from being transmitted to the drive shaft.

First, a model of the drivetrain, as shown in Fig. 1, was created to aid in the design of the controller. The damper, drive shaft, and tires, which have low rigidity relative to the other elements, are approximated as spring elements. Thus, the HV drivetrain can be approximated by the spring mass model shown in **Fig. 3**.

The nomenclature used in this figure is explained below.

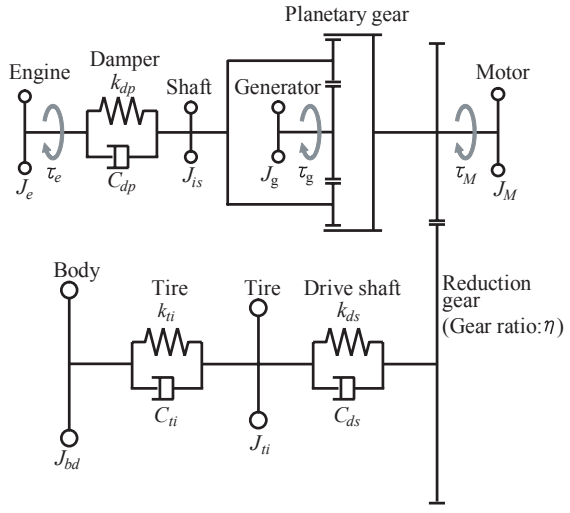

Fig. 3 Model of an HV drivetrain.

J : Inertia moment, K : Spring constant,
C : Viscous coefficient, τ : Torque,
η : Final deceleration ratio
Subscript
e : Engine, dp : Damper,
is : Input shaft, g : Generator,
M : Motor, ds : Drive shaft,
ti : Tire, bd : Body

The motor speed ω_M is expressed by Eq. (1).

$$\omega_M = G_e(s)\tau_e + G_g(s)\tau_g + G_M(s)\tau_M \quad \cdots\cdots\cdots(1)$$

where $G_e(s)$, $G_g(s)$, $G_M(s)$ are transfer functions. Engine torque τ_e is expressed separately for steady term τ_{e_cont} and ripple term $\Delta\tau_e$. And, the generator torque is expressed separately for reference torque τ_{g_ref} and compensation torque τ_{FF} as follows:

$$\tau_e = \tau_{e\_cont} + \Delta\tau_e$$
$$\tau_g = \tau_{g\_ref} + \tau_{FF} \quad \cdots\cdots\cdots\cdots\cdots(2)$$

Then, Eq. (1) can be rewritten using Eq. (2), as follows:

$$\omega_M = G_e(s)\tau_{e\_cont} + G_g(s)\tau_{g\_ref} + G_M(s)\tau_M + \{G_e(s)\Delta\tau_e + G_g(s)\tau_{FF}\} \quad \cdots\cdots(3)$$

τ_{FF} is determined such that the inside of the parentheses of the last term on the right-hand side of Eq. (3) are equal to zero.

$$\tau_{FF} = -\frac{G_e(s)}{G_g(s)}\Delta\tau_e \quad \cdots\cdots\cdots\cdots\cdots(4)$$

ω_M is not influenced by $\Delta\tau_e$, if τ_{FF} satisfies Eq. (4). In this case, the engine torque ripple is not transmitted to the drive shaft.

4. 1. 2 Engine torque ripple

The main component of the vibration prior to ignition is the engine torque ripple. Therefore, the engine torque ripple before ignition, $\Delta\tau_{e\_1}$, is used for this controller. $\Delta\tau_{e\_1}$ can be calculated using the compression/expansion of air and the inertia force of the piston.[5] $\Delta\tau_{e\_1}$ is expressed as a function of the crank angle.[9]

Figure 4 shows the calculated $\Delta\tau_{e\_1}$. Figure 4 shows that $\Delta\tau_{e\_1}$ changes sharply at a crank angle near the top dead center (TDC) of the stroke. Therefore, a highly precise crank angle is needed to perform the calculation. A highly precise crank angle can be determined using the angle sensors of the motor and generator, as follows:

$$\theta_e = \frac{1}{1+\rho}\theta_M + \frac{\rho}{1+\rho}\theta_g + \theta_{e\_ini} \quad \cdots\cdots\cdots\cdots(5)$$

Where ρ is the planetary gear ratio of the sun gear and ring gear, and θ_{e_ini} is the initial crank angle.

4. 1. 3 Compensation torque

In Fig. 2, the vibration prior to ignition is particularly large when the 2nd-order element of the engine speed is close to the resonance frequency of the damper (20 Hz). The variable gain $K_{FF}(\omega_e)$ is introduced to compensate for the torque in the vicinity of this engine speed, which is similar to the resonance frequency of the damper. Using $K_{FF}(\omega_e)$, the compensation torque of Eq. (4) is changed as follows:

$$\tau_{FF} = -K_{FF}(\omega_e)\frac{G_e(s)}{G_g(s)}\Delta\tau_{e\_1} \quad \cdots\cdots\cdots\cdots (6)$$

4. 2 Torsional vibration control

The design objective of the second controller was to change the dynamic characteristics of the drivetrain such that it does not vibrate at all.

The two-mass model shown in **Fig. 5** was used to design the controller.

Where,

J_b : Synthetic inertia moment of body and tire ($J_b = J_{bd} + J_{ti}$)

K_b : Synthetic spring constant of drive shaft and tire

$$\left(\frac{1}{K_b} = \frac{1}{K_{bd}} + \frac{1}{K_{ti}}\right)$$

C_b : Synthetic viscosity coefficients of drive shaft and tire

$$\left(\frac{1}{C_b} = \frac{1}{C_{bd}} + \frac{1}{C_{ti}}\right)$$

τ_α : Engine torque (converted into the motor axis)

θ_M : Motor angle

θ_b : Driving wheel angle (converted into the motor axis)

Here, the model shown in Fig. 5 is expressed by state Eq. (7) by taking $\omega_M = \dot{\theta}_M$, $\omega_b = \dot{\theta}_b$, $\Theta = \theta_M - \theta_b$ as the state variables.

$$\dot{x} = \boldsymbol{A}x + \boldsymbol{B}\tau_M + \boldsymbol{B}_e\tau_\alpha \quad \cdots\cdots\cdots\cdots (7)$$

$$y = [1\ 0\ 0]\,\boldsymbol{x}$$

$$\boldsymbol{x} = [\omega_M\ \ \omega_b\ \ \Theta]^T$$

$$\boldsymbol{A} = \begin{bmatrix} -\frac{C_b}{J_M\eta^2} & \frac{C_b}{J_M\eta^2} & \frac{K_b}{J_M\eta^2} \\ \frac{C_b}{J_b\eta} & -\frac{C_b}{J_b\eta} & \frac{K_b}{J_M\eta} \\ 1 & -1 & 0 \end{bmatrix}$$

$$\boldsymbol{B} = \left[\frac{1}{J_M}\ \ 0\ \ 0\right]^T, \quad \boldsymbol{B_e} = [1\ 0\ 0]^T$$

Engine torque τ_α is treated as a disturbance and the state equation, less the 3rd term on the right-hand side of Eq. (7), is used as the controller design model.

A control rule is proposed in Eq. (8), which uses torsional speed $\omega_M - \omega_b$

$$\tau_M = \tau_{M\_ref} - f(\omega_M - \omega_b) \quad \cdots\cdots\cdots\cdots (8)$$

where τ_{M_ref} is the reference motor torque, and f is the feedback gain. The gain f is determined such that both closed-loop poles become real roots so as to attain a non-vibrating characteristic, and the domination pole is set furthest from the origin in order to attain the best response characteristic.

The root locus shown in **Fig. 6** is used to

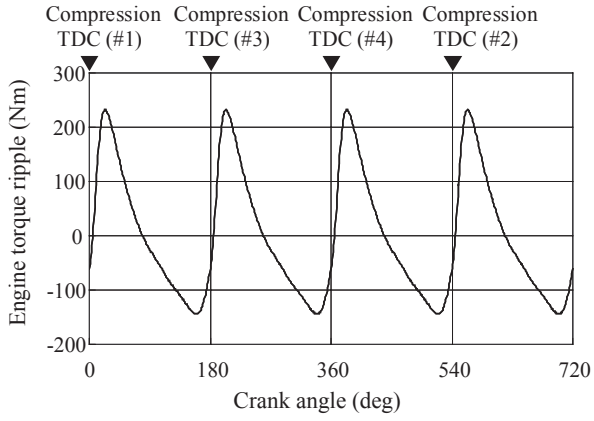

Fig. 4 Engine torque ripple at cranking.

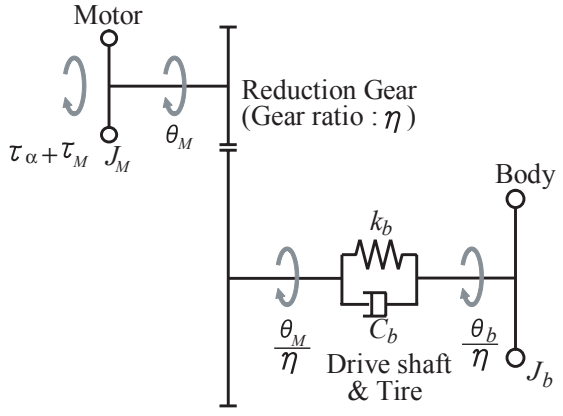

Fig. 5 Model of controller design .

determine the gain f. There are three poles in this system. One pole is always at the origin. The two other poles are a pair of complex numbers (area a in Fig. 5) which exist near an imaginary axis in an open loop ($f = 0$). When the gain f is increased, it gradually approaches a real axis, to become multiple roots on a real axis (area b in Fig. 5). Subsequently, they move on the real axis towards the origin and infinity.

From this result, the gain that realizes multiple roots satisfies the above-mentioned requirements. This gain can be uniquely calculated, as follows.

The characteristic equation of a closed loop is obtained using Eqs. (7) and (8), as follows:

$$det[s\boldsymbol{I} - (\boldsymbol{A}-\boldsymbol{B}f)] = s\left[s^2 + \left(a_1 + \frac{f}{J_M}\right)s + a_2\right] \quad \cdots\cdot(9)$$

Where

$$a_1 = \frac{C_b}{\eta}\left(\frac{1}{J_M\eta} + \frac{1}{J_b}\right)$$

$$a_2 = \frac{K_b}{\eta}\left(\frac{1}{J_M\eta} + \frac{1}{J_b}\right)$$

s = Laplace operator

The gain f that sets the poles of Eq. (9) to multiple roots is calculated as follows:

$$f = J_M\left(-a_1 + 2\sqrt{a_2}\right) \quad \cdots\cdots\cdots\cdots\cdot(10)$$

Next, we analyzed the closed loop characteristic using the gain determined using the low-dimension model and high-dimension plant model shown in Fig. 3.

Figure 7 is a Bode diagram of the transfer function from motor torque to motor speed. We found that the resonance peak of both the drive shaft and damper can be reduced using this controller, so that we could expect a reduction in the amount of vibration. The driving wheel speed ω_b is used in this controller. There is no appropriate sensor, so ω_b is estimated using a state observer.

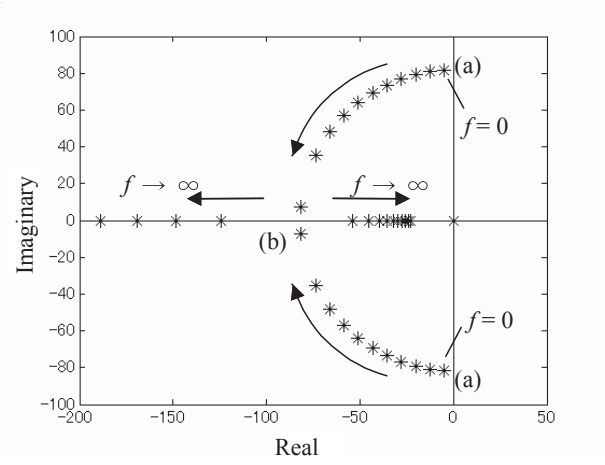

Fig. 6 Root locus.

4. 3 Application of the vibration-reducting control

Figure 8 illustrates the application of the vibration-reducting control described in this paper.

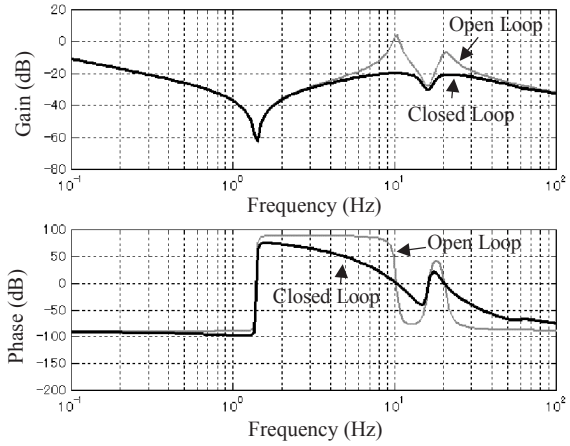

Fig. 7 Bode diagram.

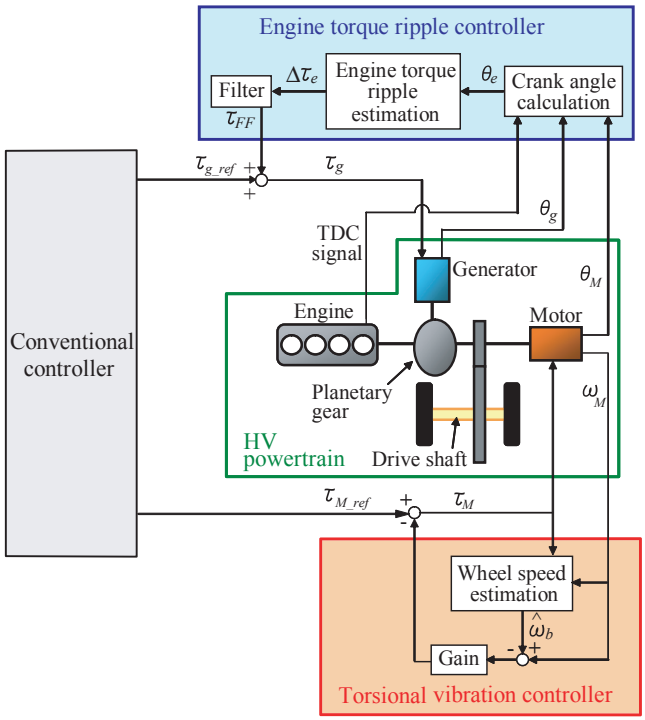

Fig. 8 Block diagram of the vibration-reducing motor control.

The vibration-reducting control is added to the conventional controller.[10)]

5. Results of experiments

We evaluated the vehicle vibration using the vibration-reducting control.

5. 1 Vibration at engine start

Figure 9 shows the floor acceleration, the generator torque, and the motor torque, normalized by the maximum torque at engine start. The proposed control method reduces the vibration in the vehicle. The peak floor acceleration with our proposed control method is only 20% of that with the conventional controller.

As a result, the passengers in the vehicle can barely detect the startup of the engine. The controller changes the generator torque and motor torque around the reference torque to reduce the engine torque ripple and the torsional vibration of the drive shaft.

5. 2 Vibration at engine stop

Figure 10 shows floor acceleration and engine speed when the engine stops. With the conventional controller, vibration occurs when the engine speed drops. With the proposed control method, however, very little vibration occurs, such that the ride comfort is greatly improved.

5. 3 Vibration at take-off with full-throttle acceleration

Vibration occurs when the driver take offs with full-throttle acceleration. This is because, in an HV, the motor traction torque can be increased more quickly than that of the ICE and engine torque is generated by the engine start.

Figure 11 shows the floor acceleration, motor torque, and motor speed at this time. The vibration that occurs immediately after take-off is reduced by the proposed control method, such that the ride comfort becomes much better. Using the proposed control method, the motor torque increases to its maximum value quickly and the motor speed does not become slow. Thus, the proposed control method successfully reduces vibration without adversely affecting the responsiveness of the motor torque.

6. Conclusion

To reduce vibration in an HV, we have devised control method for the motor and the generator. The vibration-reducting control method consists of two controllers; one to prevent the engine torque ripple

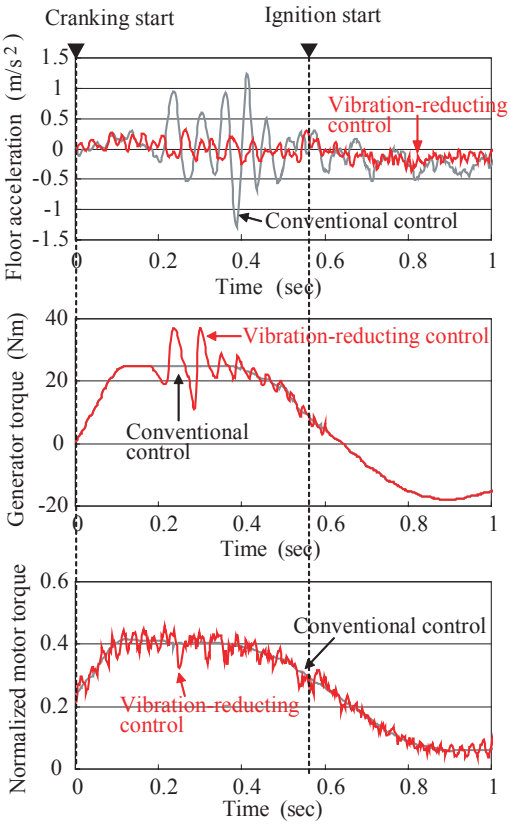

Fig. 9 Experimental results: engine start.

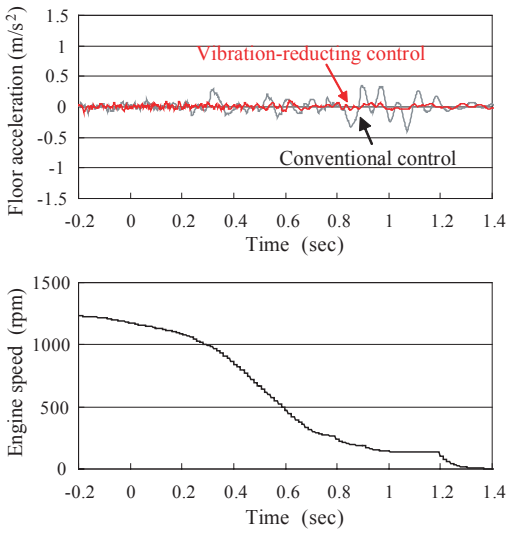

Fig. 10 Experimental results: engine stop

from being transmitted to the driving wheels, and the second to reduce the torsional vibration of the drive shaft.

Experiments showed that the control method reduces vibration and greatly improves ride comfort. This control method is achieved entirely in software.

Acknowledgments

The authors acknowledge the considerable assistance of Mr. S. Sasaki, Mr. E. Sato and other staff members at Toyota Motor Corporation.

References

1) Yoshioka, Y. and Sugita, H. : "Noise and Vibration Reduction Technology in Hybrid Vehicle Development", SAE Tech. Pap. Ser., No.2001-01-1415 (2001)
2) Moriya, K., Ito, Y., Inaguma, T. and Sato, E. : "Design of the Surge Control Method for the Electric Vehicle Powertrain", SAE Tech. Pap. Ser., No.2002-01-1935 (2002)
3) Komada, M., et al. : "Noise and Vibration Reduction Technology in New Generation Hybrid Vehicle Development", JSAE Spring Convention Proc., No.20045298(2004) (in Japanese)
4) Menne, M. and Bitscher, O. : "Comparison of Drivetrain-Oscillation Damping-Argorithms for Electric Vehicles", Proc. of 18th EVS, (2001)
5) Gotting, G. and Doncker, W. : "Comparison of Algorithms for Suppression-Control of Drivetrain-Oscillations in Electric Vehicles", Proc. of 19th EVS, (2002)
6) Davis, R. and Lorenz, R. : "Engine Torque Ripple Cancellation with an Integrated Starter Alternator in a Hybrid Electric Vehicle: Implementation and Control", IEEE Trans. on Ind. Appl., **39**-6(2003), 1765-1774
7) Takeuchi, T., et al. : "Sensibility Analysis of Vibration Transfer Path and Control of Input Force for Reduction of Acceleration and Deceleration Shock", Mitsubishi Motors tech. Rev., No. 15 (2003), 32-41
8) Sasaki, S., Takaoka, T., Matsui, H. and Kotani, T. : "Toyota's Newly Developed Electric-Gasoline Engine Hybrid Powertrain System", Proc. of 14th EVS, (1997)
9) JSAE : "Handbook of Automotive Technology (1)", (2004), 82-86 (in Japanese)
10) Kimura, A., Abe, T. and Sasaki, S. : "Drive Force Control of Two Motor Hybrid System", JSAE Spring Convention Proc., No.9832288(1998), (in Japanese)

(Report received on Mar. 28, 2005)

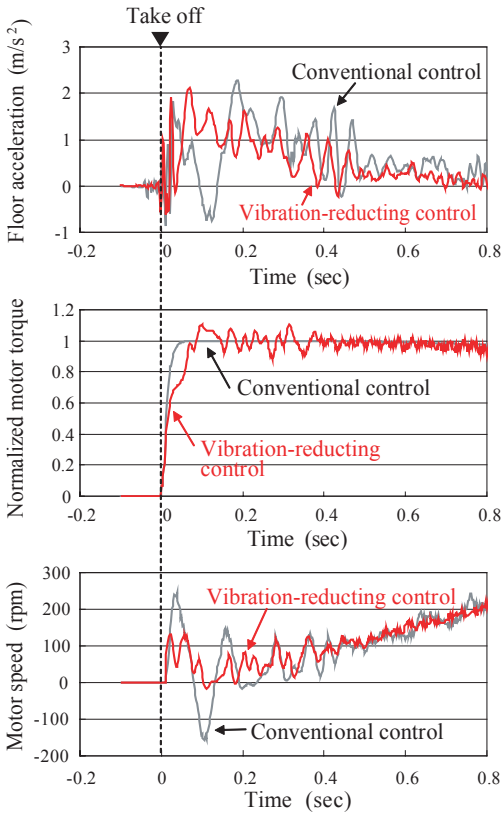

Fig. 11 Experimental results: full-throttle acceleration.

Yoshiaki Ito
Research Field : Motor control, Dynamics analysis of electric powertrain
Academic society : Soc. Instrum. Control Eng.

Shuji Tomura
Research Field : System control of hybrid vehicle
Academic society : Soc. Automot. Eng. Jpn., Soc. Instrum. Control Eng.

Kazunari Moriya
Research Field : Control of electric motors, power electronics topologies
Academic society : Inst. Electr. Eng. Jpn.